Out-of-Plane Shake-Table Tests on Unreinforced Masonry Gables

Damiani, Nicolò; Sharma, Satyadhrik; Bertassi, Marta; Smerilli, Marco; Mirra, Michele; Lanese, Igor; Parisi, Elisa Rizzo; O'Reilly, Gerard J.; Messali, Francesco; Graziotti, Francesco

Publication date
2025

Document Version
Final published version

Citation (APA)
Damiani, N., Sharma, S., Bertassi, M., Smerilli, M., Mirra, M., Lanese, I., Parisi, E. R., O'Reilly, G. J., Messali, F., & Graziotti, F. (2025). *Out-of-Plane Shake-Table Tests on Unreinforced Masonry Gables*. Paper presented at 15th Canadian Masonry Symposium 2025, Ottawa, Ontario, Canada. https://www.canadamasonrydesigncentre.com/wp-content/uploads/15th_symposium/181-Damiani.pdf

15th Canadian Masonry Symposium
Ottawa, Canada
June 2-5, 2025

Out-of-Plane Shake-Table Tests on Unreinforced Masonry Gables

Nicolò Damiani[i], Satyadhrik Sharma[ii], Marta Bertassi[iii], Marco Smerilli[iv], Michele Mirra[v], Igor Lanese[vi], Elisa Rizzo Parisi[vii], Gerard J. O'Reilly[viii], Francesco Messali[ix], and Francesco Graziotti[x]

ABSTRACT

Typical low-rise masonry buildings worldwide commonly feature unreinforced masonry (URM) walls, often paired with various pitched roof configurations supported or finished by masonry gables. These buildings constitute a significant portion of the building stock in several seismic-prone regions, including areas vulnerable to both natural and induced seismicity. Masonry gables in such buildings are frequently associated with high seismic vulnerability, as evidenced by damage observed after past earthquakes. This paper presents key results from an experimental campaign aimed at enhancing the understanding of the seismic out-of-plane response of masonry gables. Incremental full-scale shake-table tests were performed on three densely instrumented URM gables until the complete collapse. Within this context, the study systematically investigated the effects of motions applied at the top of the gable, both being linearly amplified as well as amplified and out-of-phase, with respect to the motion applied at the base of the gable. Such differential motions simulate the effect of the gable interaction with three different roof configurations, each exerting a different filtering effect on the seismic motion. The response of the gables to both induced and tectonic earthquakes was considered. The experimental findings are presented in terms of failure mechanisms, force-displacement hysteresis behaviour, and acceleration and displacement capacities. All generated experimental data, along with the associated instrumentation schemes, are openly available for download at https://doi.org/10.60756/euc-1avy7q49.

KEYWORDS

Collapse, Gable walls, Roof stiffness, Shake-table tests with differential input motions, Out of plane, Unreinforced Masonry.

[i] Postdoctoral Researcher, University of Pavia, Pavia, Italy, nicolo.damiani@unipv.it
[ii] Researcher, Delft University of Technology, Delft, The Netherlands, s.sharma-9@tudelft.nl
[iii] PhD Candidate, University School for Advanced Studies IUSS Pavia, Pavia, Italy, marta.bertassi@iusspavia.it
[iv] EUCENTRE Foundation, Pavia, Italy, marco.smerilli@eucentre.it
[v] Postdoctoral Researcher, Delft University of Technology, Delft, The Netherlands, m.mirra@tudelft.nl
[vi] EUCENTRE Foundation, Pavia, Italy, igor.lanese@eucentre.it
[vii] EUCENTRE Foundation, Pavia, Italy, elisa.rizzoparisi@eucentre.it
[viii] Associate Professor, University School for Advanced Studies IUSS Pavia, Pavia, Italy, gerard.oreilly@iusspavia.it
[ix] Assistant Professor, Delft University of Technology, Delft, The Netherlands, f.messali@tudelft.nl
[x] Associate Professor, University of Pavia, Pavia, Italy, francesco.graziotti@unipv.it

INTRODUCTION

Low-rise masonry buildings in Europe and worldwide are predominantly characterised by unreinforced masonry (URM) walls paired with various pitched roof systems, often supported by masonry gables. These structures constitute a significant proportion of the building stock in seismic-prone regions, including areas exposed to both natural seismic hazards and induced seismicity. Among their components, masonry gables are often identified as the most seismically vulnerable components in their out-of-plane (OOP) direction. Post-earthquake damage assessments worldwide provide extensive evidence of this susceptibility, which stems from several factors: their pronounced slenderness, weak connections to the roof structure, and their position at the building apex. This positioning exposes them to amplified seismic excitation compared to the motion at the ground, while they are under minimal vertical overburden loads. Moreover, the interaction between gables and flexible roof diaphragms can further increase vulnerability, as timber roof elements may amplify seismic motion rather than provide effective restraint. Despite the well-documented seismic vulnerability of URM gables, dedicated experimental studies on their seismic response [2][3] remain limited in the literature. Most available insights are derived from tests on walls with rectangular geometries [3]–[12], leaving a gap in the understanding of the specific behavior of gables under seismic loading. To address these gaps, this paper presents novel experimental findings on the dynamic seismic behaviour of densely instrumented, full-scale URM gables tested until complete collapse. The tested specimens and their detailed material characterisation are first described. Although the roof was not explicitly included in the experiments, its influence, particularly its stiffness, on the gable response is accounted for by applying differential input motions using an innovative dual shake-table setup, with one table at the gable base and another at its top. A detailed description of this experimental setup is then provided. The results of the experimental campaign are ultimately presented followed by concluding remarks.

DESCRIPTION AND MECHANICAL CHARACTERIZATION OF THE MASONRY SPECIMENS

Specimen geometry

The tested specimens consisted of identical full-scale URM gable walls, triangular in shape, with a base length of 6 m and a height of 3 m (Figure 1), and were built on a composite steel-concrete foundation. The gables were built using solid clay bricks, with average dimensions of 230 x 105 x 55 mm, resulting in a wall thickness of 105 mm. Each gable was built in 45 layers of bricks, with 10-mm-thick mortar joints.

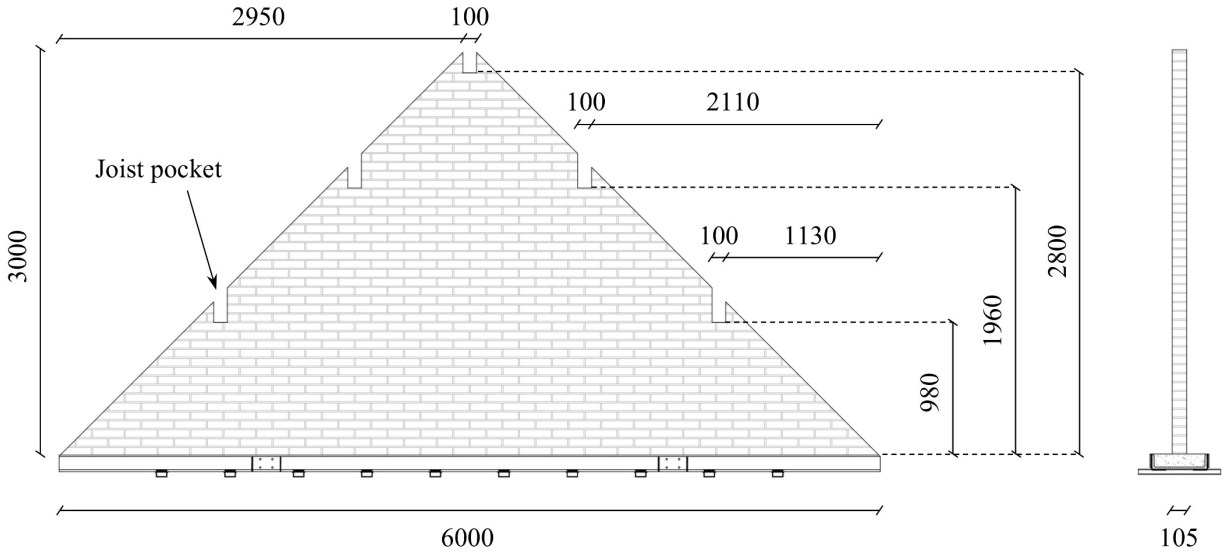

Figure 1: Full-scale masonry gable specimen details. Units of mm.

Additionally, five joist pockets were incorporated to accommodate five timber beams, with a cross-section of 100 x 200 mm. Each timber beam transferred a vertical load of 4.5 kN, resulting in a total vertical load of 22.5 kN on the gable, simulating half the weight of a typical timber roof diaphragm, consistent with the tested specimen geometry. This load corresponded to an overburden of 0.07 MPa at gable mid-height. Additionally, the beams facilitated the application of lateral loads along the height of the specimen, as further discussed in the following sections. It is worth noting that steel anchors connecting the timber joists to the masonry gables were intentionally omitted in these experimental tests. Consequently, timber-to-masonry connections relied solely on friction, corresponding to a lower bound of the seismic capacity of the gables eliminating the potential restraining effect that such connections could provide [13].

Summary of material mechanical properties

The tested gable specimens were accompanied by complementary material characterization performed on both individual constituents and masonry as a composite material. All material characterization tests were performed at the "Giorgio Macchi" Material and Structural Testing Laboratory of the Department of Civil Engineering and Architecture (DICAr) of the University of Pavia (Italy), on specimens that reached 28 days of maturation. The characterization included the compressive (f_c) and flexural strength (f_t) of mortar, the compressive (f_u) strength of bricks, the compressive strength (f_m) of masonry perpendicular to bed joints and secant elastic modulus (E_m) calculated between 10 and 33% of f_m, the bond strength (f_w) of masonry, the initial shear strength (f_{v0}) and friction coefficient (μ). All tests were performed in accordance with the latest applicable European norms [14]–[18]. Furthermore, to characterise the response of masonry bed joints under torsional shear stress ($f_{v0,tor}$, μ_{tor} evaluated assuming a linear elastic hypothesis), a dedicated test was performed [19]. The density of masonry (ρ_m) was determined from the average weight of the tested gables. Table 1 summarizes experimental mean values and coefficient of variation (C.o.V.) for the investigated mechanical properties.

Table 1: Summary of masonry, unit and mortar mechanical properties

Material properties	Symbol	Units	Mean	C.o.V.
Mortar compressive strength	f_c	[MPa]	0.68	0.26
Mortar flexural strength	f_t	[MPa]	0.20	0.50
Unit/brick compressive strength	f_u	[MPa]	42.57	0.09
Masonry compressive strength	f_m	[MPa]	7.44	0.10
Masonry elastic modulus	E_m	[MPa]	4072	0.11
Masonry initial shear strength	f_{v0}	[MPa]	0.19	-
Masonry friction coefficient	μ	[-]	0.51	-
Masonry bond strength	f_w	[MPa]	0.21	0.48
Masonry initial shear strength (torsional)	$f_{v0,tor}$	[MPa]	0.42	-
Masonry friction coefficient (torsional)	μ_{tor}	[-]	1.15	-
Masonry density	ρ_m	[kg/m^3]	1883	-

TESTING LAYOUT AND APPLIED TESTING SEQUENCE

The incremental dynamic shake-table tests on full-scale masonry gables were conducted at the EUCENTRE laboratory in Pavia (Italy), using the 9D LAB facility. This advanced seismic testing system features a dual shake-table configuration, including a top and bottom table capable of applying differential input motions covering nine degrees of freedom. While the 9D LAB in-plan dimensions (i.e., 4.8 x 4.8 m) allowed for testing a full-scale masonry gable, it could not accommodate an entire roof diaphragm structure. As a result, the influence of the roof stiffness on the seismic OOP response of the gables was accounted for by varying

the input motion imposed to the top table. In particular, within the same experimental campaign, three different configurations for the roof structure were considered: (i) Gable1-STIFF, representing a rigid roof diaphragm, where the top shake table replicated the motion of the bottom table; (ii) Gable2-SEMIFLEX, representing an intermediate case, where the top motion was linearly amplified relative to the base motion; and (iii) Gable3-FLEX, simulating a flexible roof diaphragm, leading to significant amplification and phase shift at the gable top.

Testing setup

The experimental setup consisted of a dual shake-table configuration, comprising a top and bottom table capable of applying differential input motions (Figure 2). A loading frame, assembled using tailored steel profiles, was employed to transmit accelerations along the gable height via five horizontal loading arms that were hinged to the frame. Timber beams were screwed to the steel arms to replicate the timber joists commonly found in real roof structures. It is important to notice that the loading frame was hinged at both the bottom and top shake tables to avoid introducing additional OOP stiffness and strength to the gable specimens, whose foundations were fixed to the bottom shake table using steel bolts. A stiff instrumentation frame, anchored to the bottom shake table, completed the testing setup serving as support and a fixed reference for the instruments.

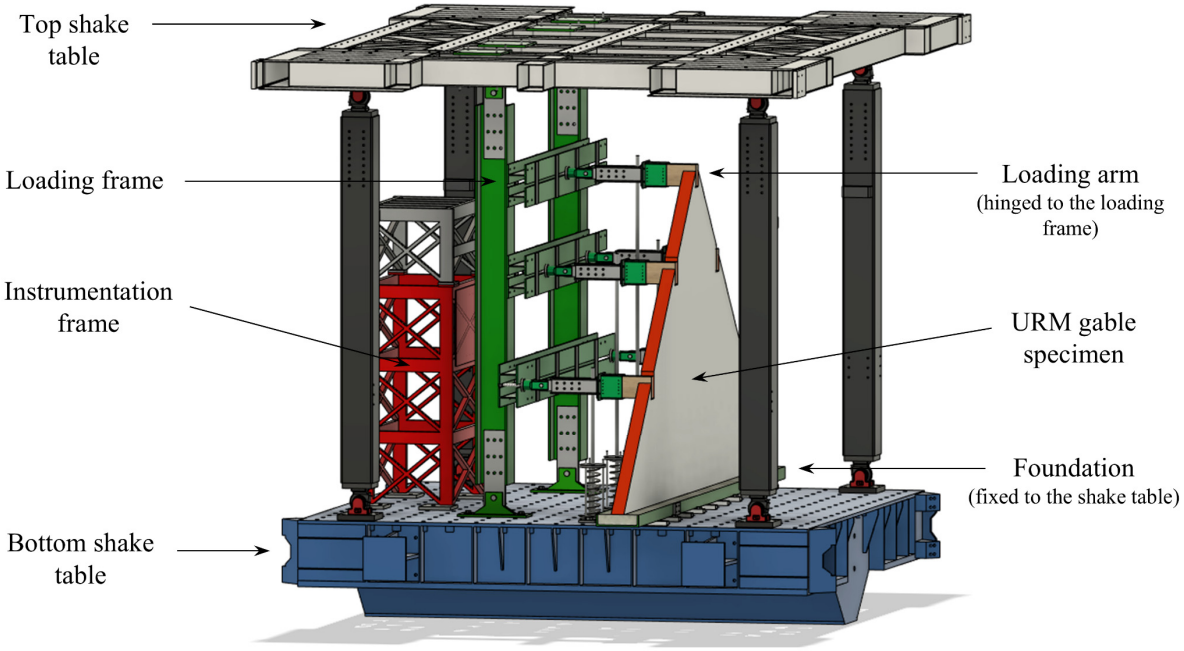

Figure 2: Three-dimensional view of the shake-table testing setup of the 9D LAB

Vertical pre-compression was applied to the gable specimens by pulling down the horizontal steel arms using steel bars in series with five springs, one per loading arm. The spring pre-compression, determined by their stiffness, generated a downward force that was transferred through the steel arms, resulting in a vertical load of 4.5 kN applied to each timber beam.

Instrumentation and data acquisition

The instrumentation adopted for each specimen included accelerometers, traditional potentiometers, wire potentiometers and a 3D optical acquisition system. The location of all the instruments was decided based on the expected deformed shapes and cracking patterns of the gables. Accelerometers were installed on the gable specimens to record acceleration-time histories, with additional accelerometers mounted on the

loading and instrumentation frames, as well as on the specimen foundation. Traditional potentiometers were used to measure the elongation or shortening of springs and the relative displacements between the timber beams and the masonry. Wire potentiometers, attached to both the loading and instrumentation frames, were used to record displacements of the gable specimens. Finally, the optical monitoring system was employed to measure displacements on the free surface of the gable, opposite to the loading frame. The complete experimental dataset, including detailed descriptions and illustrations of the instrumentation setup for each specimen, is openly available for download from the Built Environment Data database at https://doi.org/10.60756/euc-1avy7q49 [1].

Input signals and testing protocol

The 9D LAB setup allowed for the application of different input motions at the bottom and top shake tables, simulating the influence of roof diaphragm in-plane stiffness. The input motions considered two alternative floor motion (FM) scenarios, representative of both induced (FM1) and tectonic (FM2) seismicity. For the induced scenario, numerical analyses were conducted on the finite element model of a typical URM building from the Groningen region of The Netherlands. The building was analyzed in its as-built conditions with a flexible timber roof and in two retrofitted conditions: one with a stiff concrete roof, and another with a semi-flexible roof strengthened with a timber-based solution. For the tectonic seismicity scenario, recordings from the 2016 Central Italy earthquake, obtained from a monitored masonry building at the attic floor level, were used. In this case, the gable-roof interaction was modeled using a representative elastic single-degree-of-freedom system. Further details about the input signal selection can be found in [20].

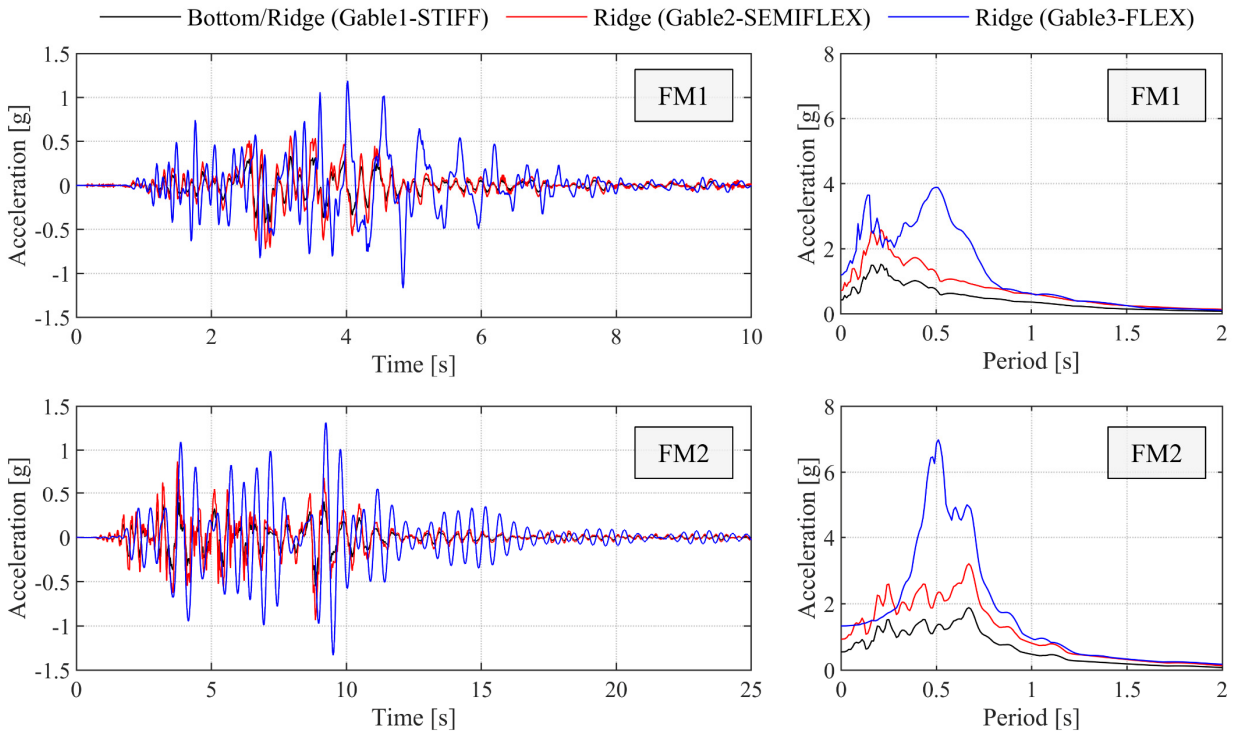

Figure 3: Summary of acceleration time histories and elastic response spectra

The induced and tectonic input signals at the bottom (i.e., attic floor) and top (i.e., ridge beam) of the gable are shown in Figure 3 along with the corresponding elastic response spectra for 5% viscous damping ratio. Table 2 lists typical intensity measures for the selected motions, including peak bottom acceleration (*PBA*), peak ridge acceleration (*PRA*), cumulative absolute velocity (*CAV*), Arias Intensity (I_A), Housner Intensity

(I_H), 5%-95% significant duration ($D_{5\text{-}95}$), period corresponding to the maximum spectral acceleration (T_d), and the maximum absolute value of the relative displacement between the ridge and the attic floor (Δ_{max}). Moreover, the sequence of input motions applied to each gable, scaling factors (SF) with respect to the signal applied at the gable bottom, and nominal and recorded values of *PBA* and *PRA* are listed in Table 3.

Table 2: Characteristics of the adopted input motions at SF = 1 [20]

Intensity measures	Induced seismicity motions			Tectonic seismicity motions		
	Attic floor*	Ridge		Attic floor*	Ridge	
	All scenarios	Semi-flexible	Flexible	All scenarios	Semi-flexible	Flexible
PBA [g]	0.42	-	-	0.54	-	-
PRA [g]	-	0.75	1.19	-	0.96	1.33
CAV [m/s]	5.35	9.48	17.6	14.3	25.3	47.2
I_A [m/s]	1.32	4.15	12.0	3.87	12.2	37.4
I_H [m]	0.95	1.69	2.24	1.41	2.50	3.44
$D_{5\text{-}95}$ [s]	2.92	2.92	4.23	7.55	7.55	10.5
T_d [s]	0.22	0.22	0.50	0.66	0.66	0.50
Δ_{max} [mm]	-	25.4	56.8	-	42.5	82.2

* The same motion was applied at the ridge in the case of the stiff roof scenario.

Table 3: Testing sequence of tested gable specimens

Test #		SF	Gable1-STIFF				Gable2-SEMIFLEX				Gable3-FLEX			
			PBA [g]		*PRA* [g]		*PBA* [g]		*PRA* [g]		*PBA* [g]		*PRA* [g]	
			Nom.	Rec.	Nom.	Rec.	Nom.	Rec.	Nom.	Rec.	Nom.	Rec.	Nom.	Rec.
1	FM1	10%	0.04	0.05	0.04	0.13	0.04	0.05	0.08	0.16	0.04	0.05	0.12	0.31
2		20%	0.08	0.08	0.08	0.19	0.08	0.08	0.16	0.29	0.08	0.09	0.24	0.53
3		30%	0.13	0.12	0.13	0.26	0.13	0.12	0.23	0.36	0.13	0.13	0.36	0.55
4		50%	0.21	0.19	0.21	0.39	0.21	0.20	0.39	0.45	0.21	0.20	0.60	0.84
5		75%	0.32	0.28	0.32	0.49	0.32	0.28	0.58	0.62	0.32	0.28	0.90	1.10
6		100%	0.42	0.37	0.42	0.61	0.42	0.38	0.78	0.81	0.42	0.36	1.20	1.33
7	FM2	50%	0.27	0.29	0.27	0.44	0.27	0.28	0.43	0.62	0.27	0.28	0.65	0.79
8		75%	0.41	0.43	0.41	0.53	0.41	0.42	0.64	0.93	0.41	0.43	0.97	1.28
9		100%	0.55	0.57	0.55	0.71	0.55	0.57	0.85	1.26	0.55	0.57	1.30	1.91
10		125%	0.69	0.69	0.69	0.84	0.69	0.71	1.06	1.46	0.69	0.70	1.62	2.34
11		150%	0.82	0.86	0.82	0.96	0.82	0.86	1.28	1.86	0.82	0.85	1.95	2.56
12		175%	0.96	1.03	0.96	1.19	0.96	1.00	1.49	2.15	-	-	-	-
13		200%	1.10	1.17	1.10	1.34	1.10	1.04	1.70	3.31	-	-	-	-
14		250%	1.38	1.51	1.38	1.64	-	-	-	-	-	-	-	-
15		300%	1.65	1.88	1.65	1.86	-	-	-	-	-	-	-	-
16		350%	1.93	1.80	1.93	2.56	-	-	-	-	-	-	-	-

RESULTS

The results of the full-scale shake-table experiments are presented and discussed in terms of damage progression throughout the incremental dynamic test sequence, the observed failure mechanisms, and the corresponding seismic capacity curves. Note that this paper focuses exclusively on the results of Gable1-STIFF and Gable3-FLEX, as they represent the two extreme cases in terms of roof flexibility.

Progression of damage and failure mechanisms

Both tested gables exhibited a one-way bending failure mechanism, with complete collapse preceded by a three-body rocking mechanism about hinges formed by two horizontal flexural cracks spanning the length of the gable at the locations of the two sets of timber joists, approximately 0.98 m and 1.96 m above the base of the gable. For all the gables, slight damage was observed after the initial test at a scaling of 10% FM1, characterized by the formation of a horizontal crack along the gable base. However, it remains unclear whether this crack was pre-existing. All cracks were identified through careful visual inspection after each test. The observed cracks are shown in Figure 4 and Figure 5, where cracks formed after the indicated test are marked in blue, while those from the preceding loading history are shown in black.

In the case of Gable1-STIFF (Figure 4), the horizontal crack connecting the lower set of joists developed before the crack connecting the upper set of joists. The lower horizontal crack first began to form during Test #13 (200% FM2), though it did not extend across the entire length of the gable. By Test #14 (250% FM2), this crack had fully developed, while the upper horizontal crack appeared in the following test, i.e., Test #15 (300% FM2). In addition to these primary horizontal cracks, a combination of stepped and horizontal cracking was also observed during these three tests, particularly around the lower set of joist pockets. The gable ultimately collapsed onto the shaking table in Test #16 (350% FM2).

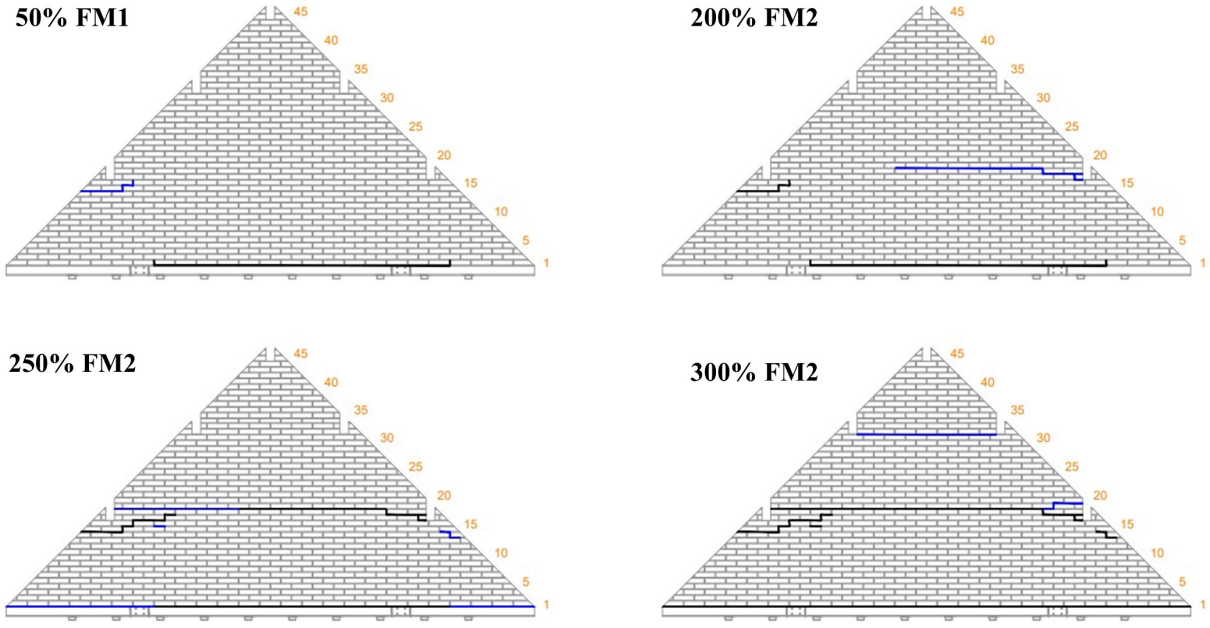

Figure 4: Progression of damage and development of failure mechanism for Gable1-STIFF

In the case of Gable3-FLEX (Figure 5), both horizontal cracks connecting the lower and upper sets of joists appeared during Test #9 (100% FM2). Two horizontal cracks formed connecting the upper set of joists, one at the bottom and the other at the top of the joist pocket. Note that, to assess the gable ability to sustain an induced seismic motion, an additional test at a scaling of 100% FM1, was conducted after this run. This test was not performed for Gable 1-STIFF. No significant increase in damage was observed, with the test only leading to the formation of an inclined stepped crack extending from the gable base to the horizontal crack that had formed during Test #5 (75% FM1). No further increase in damage was observed during Test #9 and #10 (i.e., 100% FM2 and 125% FM2). The gable ultimately collapsed onto the shaking table in Test #11 (150% FM2), much lower than the scaling factor of 350% FM2 at which Gable1-STIFF collapsed.

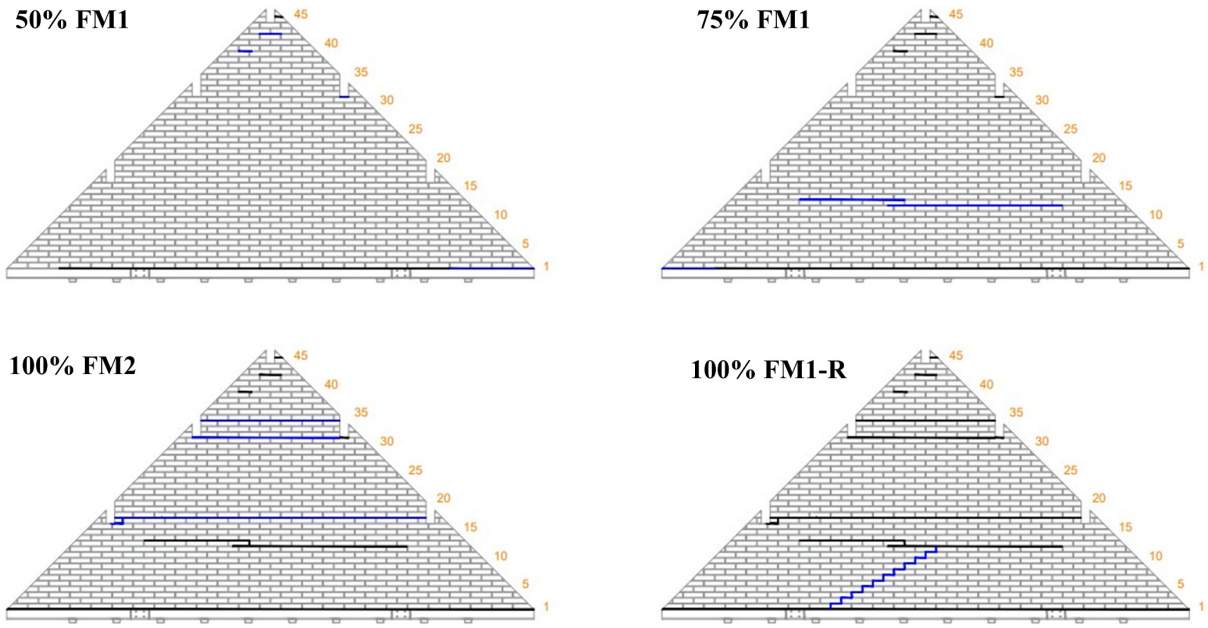

Figure 5: Progression of damage and development of failure mechanism for Gable3-FLEX

Seismic capacities

The seismic capacity of the tested gables is presented through incremental dynamic testing curves in Figure 6 and Figure 7, with two separate curves provided for each of the three gables. In the first set of curves *PBA* is plotted against the corresponding maximum displacement of the controlled point (i.e., max(d_{ctrl})) at each level of acceleration input (Figure 6a, Figure 7a). The control point displacement (d_{ctrl}) represents the maximum deflection of the gable during each run of the testing sequence, accounting for its rigid body rocking mechanism. As damage progressed, the location of this point changed, requiring trigonometric calculations to determine displacement when it was not directly instrumented. Initially positioned at the gable midpoint, it shifted accordingly once the collapse mechanism was activated. All calculations of this displacement exclude rigid displacement from the loading frame.

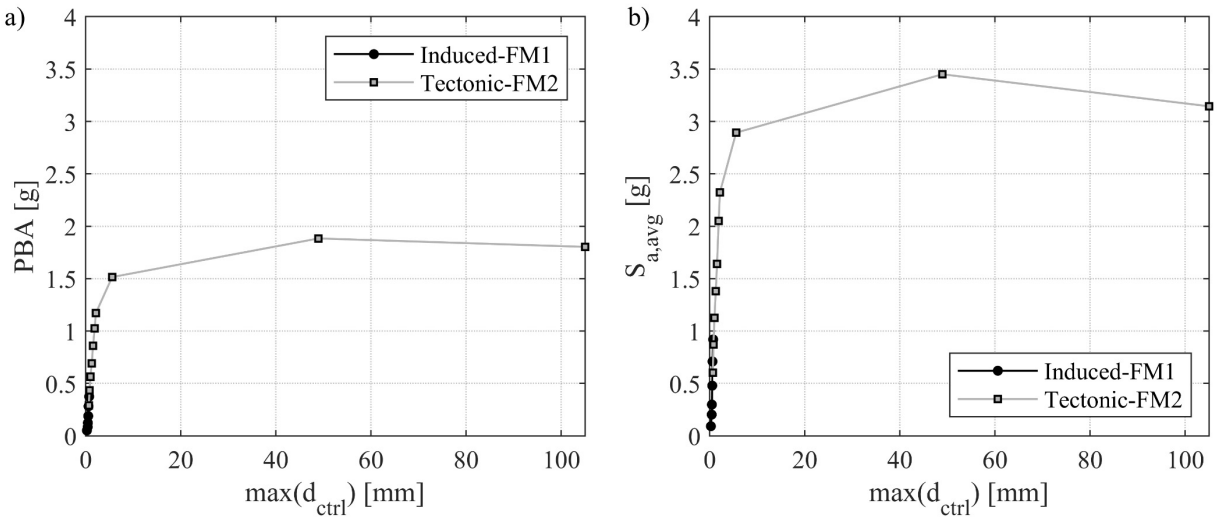

Figure 6: Capacity curves of Gable1-STIFF: a) *PBA*; b) $S_{a,avg}$.

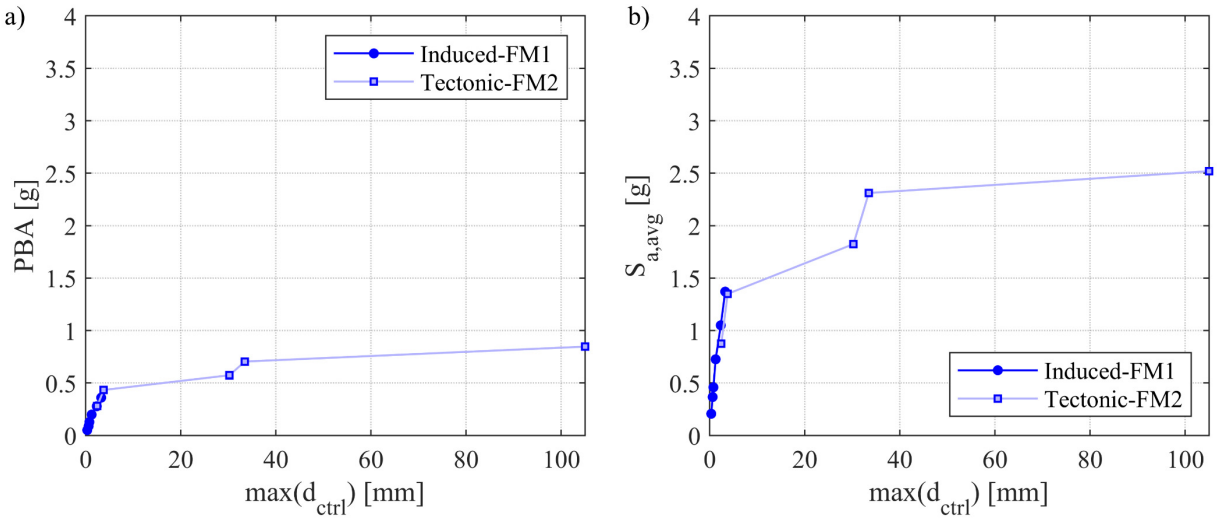

Figure 7: Capacity curves of Gable3-FLEX: a) *PBA*; b) $S_{a,avg}$.

In the second set of curves, the average spectral acceleration ($S_{a,avg}$) is plotted, calculated following the methodology of Kohrangi *et al*. [21] (Figure 6b, Figure 7b). In this case, $S_{a,avg}$ is obtained by using an acceleration time history as input for the acceleration spectra, computed as the average of the bottom table and ridge beam acceleration time histories. A period range of 0.02 s to 0.67 s is considered, corresponding to the elastic period of the gable at the start of the incremental dynamic testing sequence (~ 0.02 s) and the period at the end of the sequence (~ 0.67 s). The influence of roof flexibility on the seismic response of URM gables is evident when comparing the capacity curves in Figure 6 and Figure 7. Gable3-FLEX exhibits significantly lower seismic capacity and substantially higher flexibility, indicative of reduced stiffness compared to the other configuration.

CONCLUSIONS

This study presented the results of full-scale incremental dynamic shake-table tests on unreinforced masonry (URM) gables, focusing on their out-of-plane seismic response under different roof flexibility conditions. The experimental campaign, conducted at the EUCENTRE 9D LAB facility, implemented a dual shake-table testing methodology, enabling a detailed assessment of the effects of roof stiffness on the seismic performance of masonry gables while maintaining boundary conditions that are easily reproducible via numerical models.

The results demonstrated that interaction with the roof plays a fundamental role in the seismic response of gables. The configuration with the most flexible roof exhibited significantly lower seismic capacity, failing at a much lower floor motion intensity compared to the case with a stiff roof. The observed failure mechanisms were characterized by the formation of horizontal flexural cracks at the locations of timber joists, with ultimate collapse occurring through a three-body rocking mechanism. Furthermore, the tests highlighted how seismic amplification and phase shift effects which were more pronounced in the flexible roof configuration, increased the vulnerability of the gable.

The insights gained from this study provide valuable experimental data for refining numerical models and improving current seismic assessment methodologies for URM gables. These results can contribute to the development of enhanced predictive tools for seismic risk evaluation, particularly in regions affected by both natural and induced seismicity. Additionally, the methodologies and testing framework established in

this research may serve as a reference for future studies on masonry structures, supporting the development of improved seismic guidelines and risk mitigation strategies for URM structures worldwide.

ACKNOWLEDGEMENTS

The work presented in this paper is part of the transnational access project "ERIES-SUPREME", supported by the Engineering Research Infrastructures for European Synergies (ERIES) project (www.eries.eu), which has received funding from the European Union's Horizon Europe Framework Programme under Grant Agreement No. 101058684. This is ERIES publication number C70. Additional funds required beyond the scope of the ERIES grant for the realisation of the project were provided by the partner TNO: Netherlands Organisation for Applied Scientific Research - Nederlandse Organisatie voor Toegepast Natuurwetenschappelijk Onderzoek.

REFERENCES

[1] Damiani, N., Graziotti, F., Messali, F. and Sharma, S. (2024). "Out-of-plane shake-table tests on full-scale URM gables considering different roof configurations (ERIES-SUPREME)". *Built Environment Data*. doi: 10.60756/euc-1avy7q49

[2] Candeias, P. X., Costa, A. C., Mendes, N., Costa, A. A. and Lourenço, P. B. (2016). "Experimental assessment of the out-of-plane performance of masonry buildings through shaking table tests." *Int. J. Archit. Herit.*, 1–28.

[3] Tomassetti, U., Correia, A. A., Graziotti, F. and Penna, A. (2019). "Seismic vulnerability of roof systems combining URM gable walls and timber diaphragms." *Earthq. Eng. Struct. Dyn.*, 48, 1297–1318.

[4] Griffith, M. C., Lam, N. T. K., Wilson, J. L. and Doherty, K. (2004). "Experimental investigation of unreinforced brick masonry walls in flexure." *J. Struct. Eng.*, 130(3), 423–432.

[5] Penner, O. and Elwood, K. J. (2016). "Out-of-plane dynamic stability of unreinforced masonry walls in one-way bending: Parametric study and assessment guidelines." *Earthq. Spectra*, 32, 1699–1723.

[6] Giaretton, M., Dizhur, D. and Ingham, J. M. (2016). "Dynamic testing of as-built clay brick unreinforced masonry parapets." *Eng. Struct.*, 127, 676–685.

[7] Graziotti, F., Tomassetti, U., Penna, A. and Magenes, G. (2016). "Out-of-plane shaking table tests on URM single leaf and cavity walls." *Eng. Struct.*, 125, 455–470.

[8] Sharma, S., Tomassetti, U., Grottoli, L. and Graziotti, F. (2020). "Two-way bending experimental response of URM walls subjected to combined horizontal and vertical seismic excitation." *Eng. Struct.*, 219, 110537.

[9] Graziotti, F., Tomassetti, U., Penna, A. and Magenes, G. (2016). "Out-of-plane shaking table tests on URM single leaf and cavity walls." *Eng. Struct.*, 125, 455–470.

[10] Tomassetti, U., Grottoli, L., Sharma, S. and Graziotti, F. (2019). "Dataset from dynamic shake-table testing of five full-scale single leaf and cavity URM walls subjected to out-of-plane two-way bending." *Data Brief*, 24, 103854.

[11] Sharma, S., Grottoli, L., Tomassetti, U. and Graziotti, F. (2020). "Dataset from shake-table testing of four full-scale URM walls in a two-way bending configuration subjected to combined out-of-plane horizontal and vertical excitation." *Data Brief*, 31, 105851.

[12] Tondelli, M., Beyer, K. and DeJong, M. (2016). "Influence of boundary conditions on the out-of-plane response of brick masonry walls in buildings with RC slabs." *Earthq. Eng. Struct. Dyn.*, 45(8), 1337-1356.

[13] Correia, A. A., Tomassetti, U., Campos Costa, A., Penna, A., Magenes, G. and Graziotti, F. (2018). "Collapse shake-table test on a URM-timber roof substructure." *Proc., 16th European Conf. on Earthquake Engineering (16ECEE)*, Thessaloniki, Greece, 18–21.

[14] European Committee for Standardization (CEN). (2006). *Methods of test for mortar for masonry. Part 11: Determination of flexural and compressive strength of hardened mortar.* European Standard EN 1015-11, Brussels, Belgium.
[15] European Committee for Standardization (CEN). (2011). *Methods of test for masonry units. Part 1: Determination of compressive strength.* European Standard EN 772-1, Brussels, Belgium.
[16] European Committee for Standardization (CEN). (1998). *Methods of test for masonry. Part 1: Determination of compressive strength.* European Standard EN 1052-1, Brussels, Belgium.
[17] European Committee for Standardization (CEN). (2005). *Methods of test for masonry. Part 5: Determination of bond strength by the Bond Wrench method.* European Standard EN 1052-5, Brussels, Belgium.
[18] European Committee for Standardization (CEN). (2007). *Methods of test for masonry units. Part 3: Determination of initial shear strength.* European Standard EN 1052-3, Brussels, Belgium.
[19] Sharma, S., Graziotti, F. and Magenes, G. (2021). "Torsional shear strength of unreinforced brick masonry bed joints." *Constr. Build. Mater.*, 275, 122053.
[20] Mirra, M., Damiani, N., Sharma, S., Graziotti, F. and Messali, F. (2025). "Input motion definition for two-level shaking table testing of gable walls in unreinforced masonry buildings with different roof typologies." *Structures*. Submitted in November 2024.
[21] Kohrangi, M., Bazzurro, P., Vamvatsikos, D. and Spillatura, A. (2017) "Conditional spectrum-based ground motion record selection using average spectral acceleration." *Earthq. Eng. Struct. Dyn.*, 46: 1667–1685.